CLIMATE-DRIVEN SHIFTS IN SNOWPACK CONDITIONS FAVORABLE FOR WET SNOW AVALANCHES: INSIGHTS FROM SNOW COVER MODEL SIMULATIONS

Andrea Bruckmeier*[1], Christoph Mitterer[2], Karl Birkeland[3], Eric Sproles[1,4], Erich Peitzsch[5,1]

[1]*Department of Earth Sciences, Montana State University, Bozeman, Montana, USA*
[2]*Avalanche Warning Service Tirol, Land Tirol, Innsbruck, Austria*
[3]*Birkeland Snow and Avalanche Scientific, Bozeman, Montana, USA*
[4]*Geospatial Core Facility, Montana State University, Bozeman, Montana, USA*
[5]*U.S. Geological Survey, Northern Rocky Mountain Science Center, West Glacier, Montana, USA*

ABSTRACT: Forecasting wet snow avalanches remains a major challenge due to their temporal and spatial variability. Long-term climate trends are producing more variable and extreme weather, creating conditions outside historical experience, and increasing forecasting uncertainties. To assess how climate change affects the frequency and timing of wet snow avalanches, we examined the long-term conditions that support wet snow formation. Specifically, we ask: Will the onset of wet snow avalanche conditions or season end shift toward the mid century? And will maximum snow height decrease in avalanche starting zones? To address these questions, we analyze long-term snow cover simulations across our study site in Glacier National Park, Montana, located in an intermountain snow climate. We examined trends in simulated snow depth, and timing of liquid water infiltration over the past four decades (1979–2023) using a physically based snow cover model. To force the model with meteorological data, we use the long-term regional hydroclimate reanalysis dataset U.S. Geological Survey CONUS404 with 4 km spatial resolution and 1h temporal resolution. The use of gridded meteorological inputs to drive a one-dimensional point model introduces inherent scale mismatches. To address this limitation, we use multiple grid points within the study area to simulate a more representative, generalized snowpack, and filter the grid points based on elevation to distinguish between upper- and mid-elevation starting zones. Finally, we analyzed shifts in snow depth, melt-out-day, and LWC_{index} (bulk liquid water content (LWC) normalized by the residual water content). We use snow depth as a proxy for changes in slab thickness, the LWC_{index} as an indicator of wet snow avalanche conditions, and melt-out date as a measure of shifts in season length. We ran simulations on flat terrain and on north- and south-facing virtual slopes (38°), across mid-elevation (1,600–1,900 m) and upper-elevation ($\geq$1,900 m) sites for the historical dataset as baseline and a Pseudo-Global-Warming (PGW) dataset to identify a warming driven shift. Across all aspects and both elevation bands, PGW forcing produces a consistent reduction in annual maximum snow depth (median shift -0.15 to -0.26 m, $p < 0.001$) over 44 seasons, with the largest reductions on north-facing slopes and a modest but significant strengthening of this reduction over the 44-year simulated record. Melt-out starts 10–14 days earlier under PGW across all aspect–elevation combinations ($p < 0.001$), again most pronounced on north-facing, higher-elevation terrain. The LWC_{index} threshold-crossing dates likewise shift earlier under PGW, indicating an earlier onset of wet snow avalanche conditions across the domain. Together, these results point to a snowpack that is both thinner and wetter earlier in the season under future warming, with the strongest signal consistently on north-facing slopes at higher elevation. This work lays the groundwork for climate-informed forecasting and mitigation and offers historical context for avalanche operations in a changing climate. Understanding long-term trends can help avalanche professionals interpret current observations, improve wet snow avalanche forecasting, and develop more effective mitigation strategies in a warming climate.

KEYWORDS: SNOWPACK, wet snow, snow depth, PGW, long-term trends, avalanche forecasting

1. INTRODUCTION

Rising air temperatures affect snow accumulation and melt processes across mountain regions, resulting in reduced snow depth and earlier melt-onset (Hale et al. 2023; Newton et al. 2021). These changes affect the timing, magnitude, and character of avalanche activity, creating new challenges for avalanche forecasting and risk management (Hao et al. 2023; Peitzsch et al. 2021).

Recent studies have documented a growing proportion of wet snow avalanches in mountain regions, often associated with earlier melt onset and more frequent rain-on-snow events, whereas an increase in temperatures decreases the size and number of avalanches, particularly in lower elevations (Eckert et al. 2024; Mayer et al. 2024; Peitzsch et al. 2021; Pielmeier et al. 2013). In

* *Corresponding author address:*
Andrea Bruckmeier, Montana State University, Department of Earth Sciences
Traphagen Hall 126, Bozeman MT-59717
email: andrea.bruckmeier@montana.edu

the western United States, evidence is emerging of shifting avalanche patterns. A tree-ring based avalanche chronology in northwest Montana shows that years with large and destructive avalanches have become less frequent since the mid-20th century (Peitzsch et al. 2021). Specifically, the probability of large avalanche cycles declined by roughly 14% between 1950 and 2017, coinciding with warming and a decrease in snow cover in that region. Historically, the largest avalanche winters in Montana were associated with exceptionally stormy, snow-rich conditions. However, in recent decades, major avalanche cycles have also been increasingly linked to higher temperatures and a thinner snow cover (Peitzsch et al. 2021). This indicates a shift in the primary drivers of avalanche activity, such as a change in snowpack structure and weather patterns that align with observations of unusual mid- to late-winter avalanche cycles in the Rocky Mountains triggered by storms (Peitzsch et al. 2025).

Climate projections in other regions suggest that warming will continue throughout the 21st century, indicating an earlier occurrence of wet snow avalanche cycles each year (Castebrunet et al. 2014; Eckert et al. 2024; Lazar and Williams 2008; Reuter et al. 2025). Model-based studies indicate an earlier onset of melt, more frequent rain-on-snow events, and an increasing likelihood of wet snow avalanche activity at elevations that currently experience predominantly dry snow conditions in the European Alps (Castebrunet et al. 2014; Eckert et al. 2024; Kruyt et al. 2023; Mayer et al. 2024). Simulations for Aspen Mountain in Colorado projected that by 2030 wet snow avalanches would start 2 to 19 days earlier each spring (compared to late-20th century norms), with advances of up to 6 to 22 days at lower mountain elevations. By 2100, under mid-range warming scenarios, wet snow avalanches on Aspen Mountain could occur 3–4 weeks earlier than historic averages, and under a high-emission scenario, the wet snow avalanche season might begin 6–9 weeks earlier (Lazar and Williams 2008). These projections illustrate how climate drivers can shift the timing of wet snow avalanches further into periods that have typically been associated with dry avalanche activity.

Long-term observational avalanche records remain limited. Datasets are often short, spatially discontinuous, and capture avalanche occurrence and size rather than the underlying snowpack state that governs wet snow instability. This likely explains why several of the studies above (e.g., Castebrunet et al. 2014; Lazar and Williams 2008; Eckert et al. 2024) rely on modeled rather than observational data. Thus, physics-based snow cover models offer a proxy to examine multi-decadal changes in snowpack evolution and melt processes directly relevant to wet snow avalanche conditions. Here, we use 1-D physics-based SNOWPACK simulations (Bartelt and Lehning 2002) forced with the CONUS404 hydroclimate reanalysis dataset to investigate historical and future trends (Rasmussen et al. 2023; Xue et al. 2024) in snow depth, melt-out timing, and liquid water infiltration in Glacier National Park, Montana, with the intention to improve our understanding of how increasing air temperatures can influence snow conditions that govern wet snow avalanche activity.

2. METHODS

2.1. Glacier National Park

Our study site is Glacier National Park, Montana, USA. The park is located in northwest Montana and borders Canada at its north end. It encompasses about 4,100 km^2 including more than 175 mountain peaks along the Continental Divide and a vertical relief of 2,100 m. Therefore, precipitation varies throughout the park: the drier areas on the east side of the Continental Divide receive an average yearly precipitation of 584 mm/year whereas wetter areas on the west side get 762 mm/year and in isolated micro-climates up to 2,540 mm/year (National Park Service 2026). The snow climate in this region is classified primarily as intermountain. It is occasionally influenced by maritime air masses during specific weather patterns, placing it near the transitional zone between intermountain and coastal snow climates (Mock and Birkeland 2000).

2.2. CONUS404 and CONUS404 PGW datasets

The U.S. Geological Survey CONUS404 dataset provides a high-resolution (4 km), hourly hydroclimate reanalysis covering the conterminous United States from water years 1979 through 2023 (Rasmussen et al. 2023). It includes key atmospheric and land-surface variables such as precipitation, air temperature, wind, and radiation, dynamically downscaled from ERA5 reanalysis using the Weather Research and Forecasting model (WRF) and Noah-Multiparameterization land-surface model (He et al. 2023; Hersbach et al. 2020). Its counterpart, the U.S. Geological Survey CONUS404 Pseudo-Global-Warming (PGW) dataset, leverages the same modeling framework but incorporates climate perturbations derived from Community Earth System Model version 2 Large Ensemble (CESM2-LENS2) projections (Xue et al. 2024). CESM2-LENS2 comprises 100 independent ensemble members at 1° resolution, covering historical (1850–2014) and future (2015–2100) periods under the CMIP6 SSP3-7.0 scenario, providing robust estimates of internal climate variability and anthropogenic climate change (Rodgers et al. 2021). SSP3-7.0 represents a medium-to-high but not worst-case pathway reaching roughly 7.0 W m^{-2} of radiative forcing by 2100 (O'Neill et al. 2016; Riahi et al. 2017). The PGW method changes the atmospheric state to represent plausible future warming scenarios, and is descriptive more than diagnostic. It enables evaluation of climate-driver impacts that are designed to preserve an identical day-by-day synoptic evolution, with a climate-warming delta applied to the thermodynamic boundary forcings. In this way, PGW isolates the thermodynamic warming signal while keeping synoptic variability fixed (Brogli et al. 2023). Together, the CONUS404 and CONUS404 PGW datasets offer insight into how historical events might unfold under a warmer climate, capturing scenario-based variability within the 1979–2023 period.

2.3. SNOWPACK simulations

To simulate snow cover over 44 seasons (1979 - 2023), we used the physically based 1-D snow cover model SNOWPACK (Lehning et al. 2002; Bartelt and Lehning 2002; Wever et al. 2014; WSL Institute for Snow and Avalanche Research SLF 2026). We forced the model with meteorological variables from the CONUS404 and CONUS404 PGW datasets at a spatial resolution of 4 km, including precipitation, wind, incoming long- and shortwave radiation, air temperature and relative humidity. For the water transportation scheme, we used bucket mode (Bartelt and Lehning 2002; Wever et al. 2015). SNOWPACK solved the full surface energy balance at the snow–atmosphere interface using a Neumann boundary condition. The model derived wind speed and direction from the U (west-to-east zonal wind) and V (south-to-north meridional wind) components provided by the climate datasets.

We simulated snow cover for grid cells within two elevation bands: mid-elevations (1,600–1,900 m) and high elevations (>1,900 m). The high-elevation band included 91 grid cells (1,456 km^2), whereas the mid-elevation band included 80 grid cells (1,280 km^2). For each grid cell, we simulated one flat-field configuration and two virtual slopes with a 38° inclination representing north- and south-facing aspects.

We evaluated model performance by comparing simulations with SNOWPACK runs using Logan Pass weather observations and Flattop Mountain SNOTEL snow depth data for the 2019–2021 winters (Synoptic Data PBC 2026; USDA Natural Resources Conservation Service 2026). Through sensitivity testing, we reduced wind speeds in the CONUS404 data by 20% to improve agreement between CONUS404-driven and weather station-driven snowpack outputs.

2.4. Data analysis

We compared historical and PGW simulations using a paired design where we matched seasons by their relative chronological position within each 44-year record. For each grid cell, elevation band, and terrain aspect, the PGW–historical shift was tested against zero using a one-sample Wilcoxon signed-rank test on each grid cell's own across-season median shift (Wilcoxon 1945). Negative values indicate either an earlier date in the season or a smaller snow depth, depending on the metric shown. Maximum snow height (HS_{max}) represents the seasonal maximum snow depth. Melt-out day was the first day on or after 1 February on which snow height permanently returned to zero. LWC_{index} is the bulk LWC normalized by the residual water content, defined as a constant volumetric LWC of 0.03 (3 vol.%), following Mitterer et al. (2013). For each season, we identified the first day the index exceeded 0.3 and 1.0 indicating potential wet snow avalanche activity early (0.3) and later (1.0) in the season (Mitterer et al. 2016).

3. RESULTS

3.1. Seasonal maximum snow height

PGW forcing reduced HS_{max} across all three terrain aspects and both elevation bands ($p < 0.001$ throughout; Fig. 1) when compared to historical simulations. The reductions were the smallest on flat terrain (median shift $\Delta = -0.15$ m at 1,600–1,900 m, $\Delta = -0.18$ m at $\geq$1,900 m) and the largest on north-facing slopes ($\Delta = -0.24$ m and -0.26 m, respectively), with south-facing slopes intermediate ($\Delta = -0.18$ m in both elevation bands). At every aspect and elevation combination, the upper-elevation band showed a larger reduction than the mid-elevation band. Within the PGW scenario, a small but statistically significant negative trend at both elevation bands exists (1,600–1,900 m: slope $= -0.0013$ season^{-1}, $n = 3,510$, 80 cells; $\geq$1,900 m: slope $= -0.0012$ season^{-1}, $n = 4,004$, 91 cells; $p < 0.001$ both; Fig. 2), indicating that the PGW-driven reduction in HS_{max} intensifies over the 44-year simulated record rather than remaining constant.

3.2. Melt-out day

Melt-out date arrives significantly earlier in the year under PGW forcing across all three terrain aspects and both elevation bands ($p < 0.001$ throughout; Fig. 3) when compared to the historical period. Advances were similar on flat terrain (median shift $\Delta = -10.5$ days at 1,600–1,900 m, $\Delta = -11.5$ days at $\geq$1,900 m) and south-facing slopes ($\Delta = -10.0$ days and -11.5 days). North-facing slopes showed the largest advance of the three aspects at both elevation bands ($\Delta = -12.5$ days and -14.0 days). As with HS_{max}, the upper-elevation band showed a larger advance than the mid-elevation band at every aspect.

3.3. LWC_{index}

The date on which the LWC_{index} first exceeded both thresholds (0.3 and 1.0) advanced significantly under PGW forcing across all three terrain aspects, both elevation bands, and both thresholds ($p < 0.001$ throughout; Fig. 4). The advances were the greatest for the $LWC_{index} = 0.3$ threshold at the upper elevation band, ranging from $\Delta = -12.0$ days (south) to $\Delta = -16.5$ days (flat) to $\Delta = -22.0$ days (north), and smaller for the $LWC_{index} = 0.3$ threshold at the mid-elevation band ($\Delta = -7.0$ to -13.8 days). Advances in the $LWC_{index} = 1.0$ threshold were more consistent across aspects and elevation bands ($\Delta = -12.8$ to -17.5 days) than those in the $LWC_{index} = 0.3$ threshold. As with HS_{max} and melt-out date, the upper-elevation band showed a larger advance than the mid-elevation band at every aspect and threshold, and north-facing slopes showed the largest advances of the three aspects for both thresholds.

4. DISCUSSION

In this study, we investigated the effects of PGW on HS_{max}, melt-out day, and LWC_{index} over 44 simulated seasons. Across north-facing, south-facing, and flat-field simulations in both elevation bands (1,600–1,900 m and $>$1,900 m), HS_{max} decreased and melt-out day and LWC_{index} showed an earlier onset within the season. These findings align with other studies in the Rocky Mountains, which similarly report decreasing snow heights and earlier onset of wet snow conditions (Peitzsch et al. 2021; Lazar and Williams 2008).
In particular, the PGW-driven shift was greatest on north-facing slopes across all three variables, with a maximum shift of -22 days for LWC_{index} = 0.3 on high elevation compared to -12 days on south-facing slopes. Although this result may seem counterintuitive, because snowmelt is generally understood to depend strongly on solar radiation, a possible explanation is that each aspect starts from a different baseline. South-facing slopes already receive a lot of solar input, meaning that more warming adds only a small additional effect. North-facing slopes get less sun-exposure and rely more on air temperature to drive melt (Evan and Eisenman 2021).
Most existing studies focus on elevation-dependent changes (Mayer et al. 2024; Eckert et al. 2024; Lazar and Williams 2008); comparatively few examine slope-aspect dependencies (López-Moreno et al. 2014). Our results contrast with those of the Pyrenees, where snowpack duration and annual maximum accumulation were more sensitive to warming on southerly than northerly aspects (López-Moreno et al. 2014). A plausible explanation could be the regional difference in latitude (Glacier National Park: $\sim 48.75°$ N; Pyrenees: $\sim 42.5°$ N). Lower winter air temperatures plus more low-sun-angle shading may make north-facing slopes in Glacier National Park more temperature-reliant relative to south-facing ones (National Park Service 2026; Buisan et al. 2016). As Mayer et al. (2024) note, aspect dependencies under a changing climate remain understudied, in part because models introduce substantial uncertainty in how they resolve wind redistribution.
A decrease in HS_{max} within avalanche starting zones does not necessarily imply reduced avalanche activity. Shallower snowpacks are frequently more prone to faceting and the formation of persistent weak layers (Hägeli and McClung 2003). Our finding that high-elevation starting zones are more affected by snow-depth reduction than lower-elevation bands again differs from results in the Swiss Alps, where high elevations are projected to retain more solid precipitation under warming (Eckert et al. 2024).
For the LWC_{index} thresholds, we note that PGW forcing advances both thresholds. For LWC_{index} = 0.3, this means, that wet snow avalanche conditions occur earlier in the season but also are more inter-annually variable. This threshold usually marks the first wet cycle of the season potentially representing rain-on-snow events or early-season warm ups (Mitterer et al. 2013). LWC_{index}=1.0 often marks the second cycle of

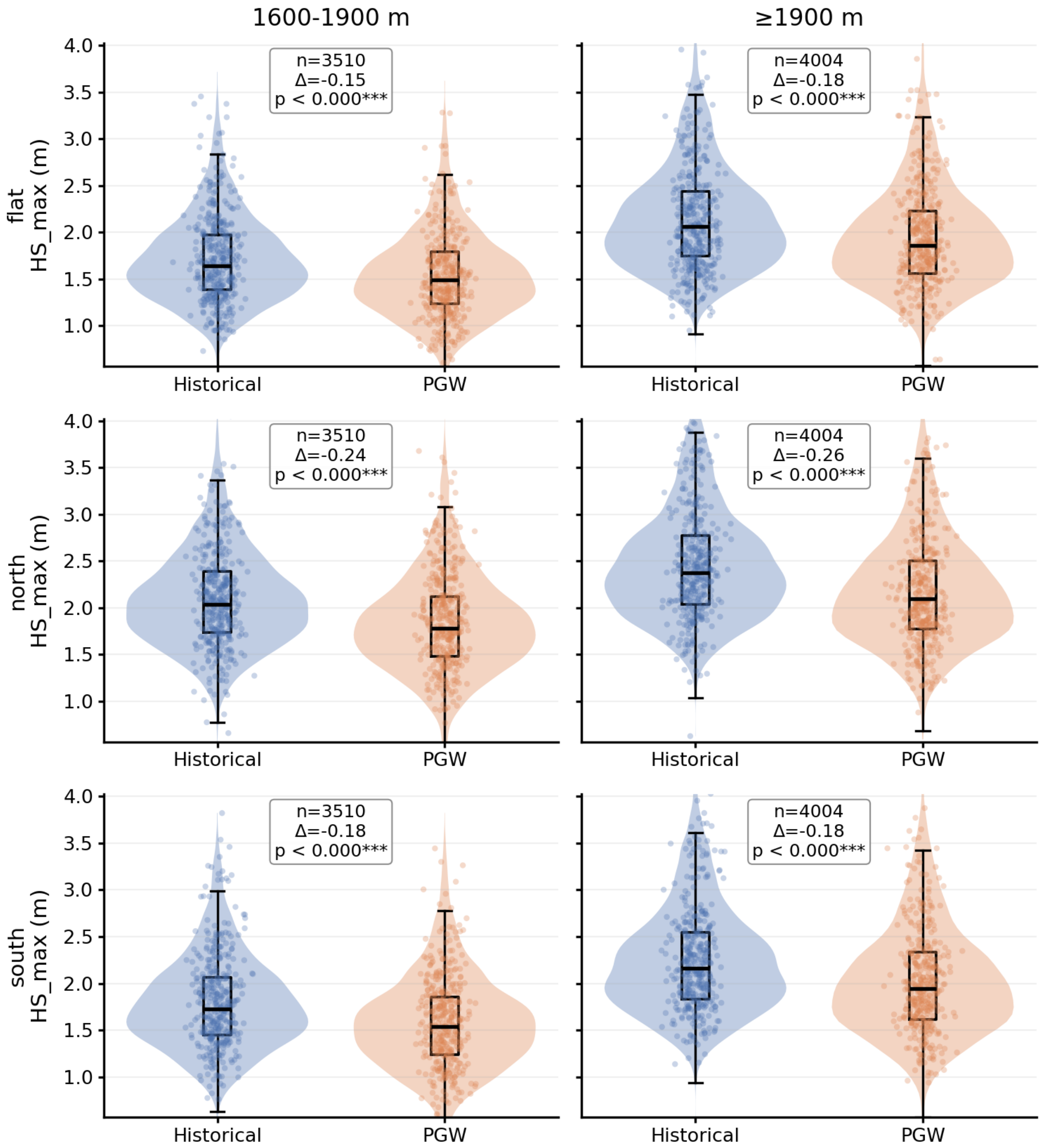

Figure 1: Distributions of annual maximum snow height (HS_{max}) under historical (blue) and PGW (orange) simulations, for three terrain aspects (flat, north-facing, south-facing; rows) and two elevation bands (1,600–1,900 m, ≥1,900 m; columns). Each panel shows a violin (kernel density) with an overlaid boxplot and a jittered strip of individual grid-cell/season values pooled across all 44 matched seasons; the shared y-axis spans the 0.5th–99.5th percentile of the pooled data. Inset text reports the pooled sample size (n), the median PGW−historical shift (Δ) in meters, and the p-value from a one-sample Wilcoxon signed-rank test on each grid cell's own across-season median shift. All six panels show a significant reduction in HS_{max} under PGW ($\Delta = -0.15$ to -0.26; $p < 0.001$), largest on the north-facing aspect at both elevation bands.

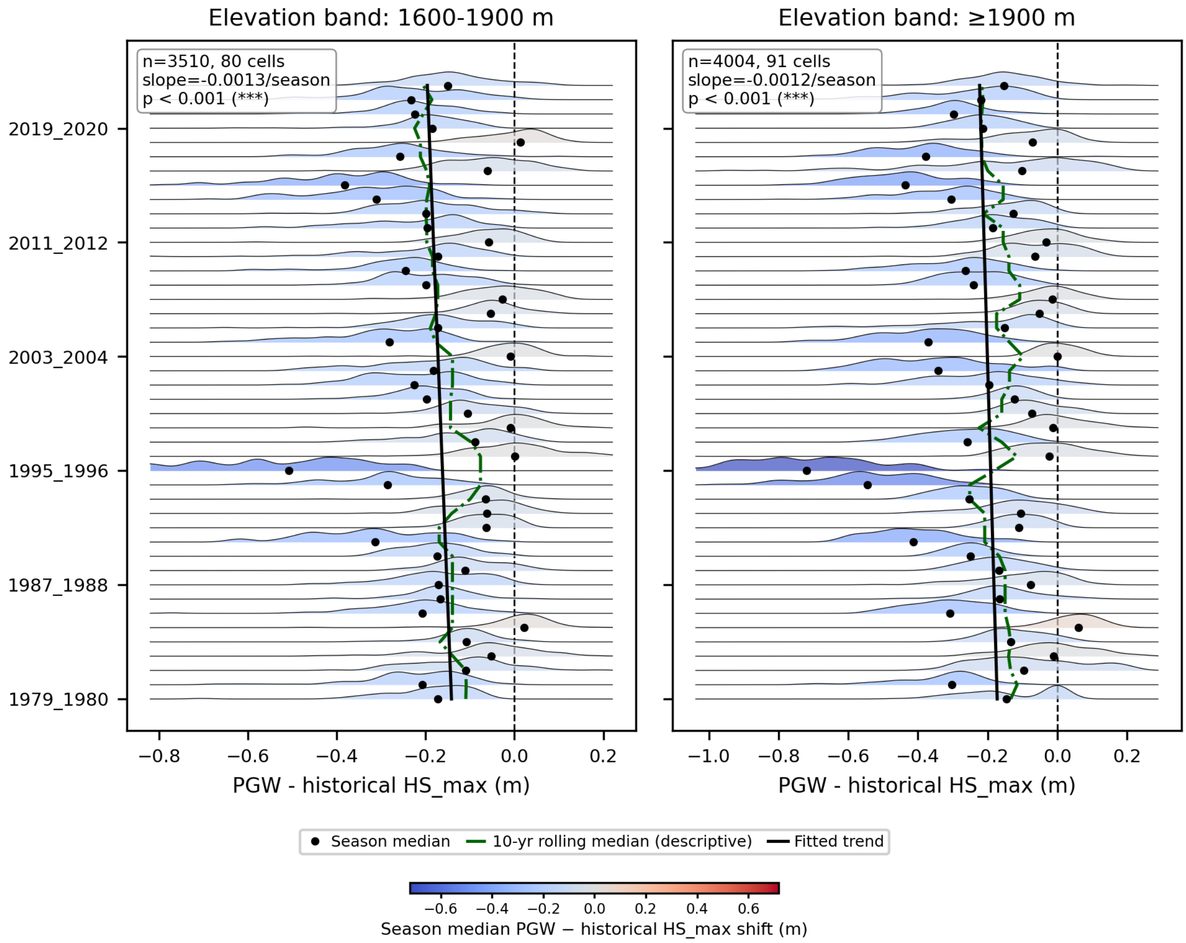

Figure 2: Year-by-year distribution of the per-grid-cell PGW−historical shift in annual maximum snow height (HS_{max}), flat-field terrain, for the lower (1,600–1,900 m; left) and upper ($\geq$1,900 m; right) elevation bands. Each ridge shows the kernel density of the shift across grid cells for one simulated season. Black dots mark season medians; the dash-dotted green line is a 10-year rolling median (descriptive only). The solid black line is the fitted trend from a linear mixed-effects model (shift $\sim$ year, random intercept per cell). Both bands show a significant negative trend (lower: $n = 3,510$, 80 cells, slope $= -0.0013$ season^{-1}; upper: $n = 4,004$, 91 cells, slope $= -0.0012$ season^{-1}; $p < 0.001$ both), indicating the PGW-driven reduction in HS_{max} grows over the simulated record.

the season symbolizing primarily melt-induced warm-ups in the spring (Mitterer et al. 2016). The advances in wet snow conditions agree with findings from Aspen, Colorado, despite differences in their identification (Lazar and Williams 2008). Studies from the European Alps likewise report earlier and increasing wet snow avalanche activity at high elevations, supporting our results (Mayer et al. 2024; Eckert et al. 2024; Reuter et al. 2025).

Our results should be interpreted as descriptive rather than diagnostic. PGW perturbs the thermodynamic profile but largely preserves circulation. As a result, dynamical responses, such as shifts in storm frequency, track, or wind patterns, are not represented (Brogli et al. 2023; Xue et al. 2023). Adachi et al. (2017) found that this storm-to-storm variability, when held fixed, can even exceed the mean climate shift itself. This effect is larger in smaller domains, like ours. Fixed circulation also means wind-driven redistribution, a main driver of aspect-dependent accumulation, is not resolved by our approach. Still, PGW has advantages over fully dynamically-downscaled projections: because it reuses observed weather patterns, it avoids much of the model bias that comes from a simulated circulation and these short term meteorological patterns drive snowpack structure and avalanche formation (Brogli et al. 2023; Xue et al. 2023). By isolating temperature change from circulation change, PGW targets the mechanism tied to our outcome: warming drives snowmelt

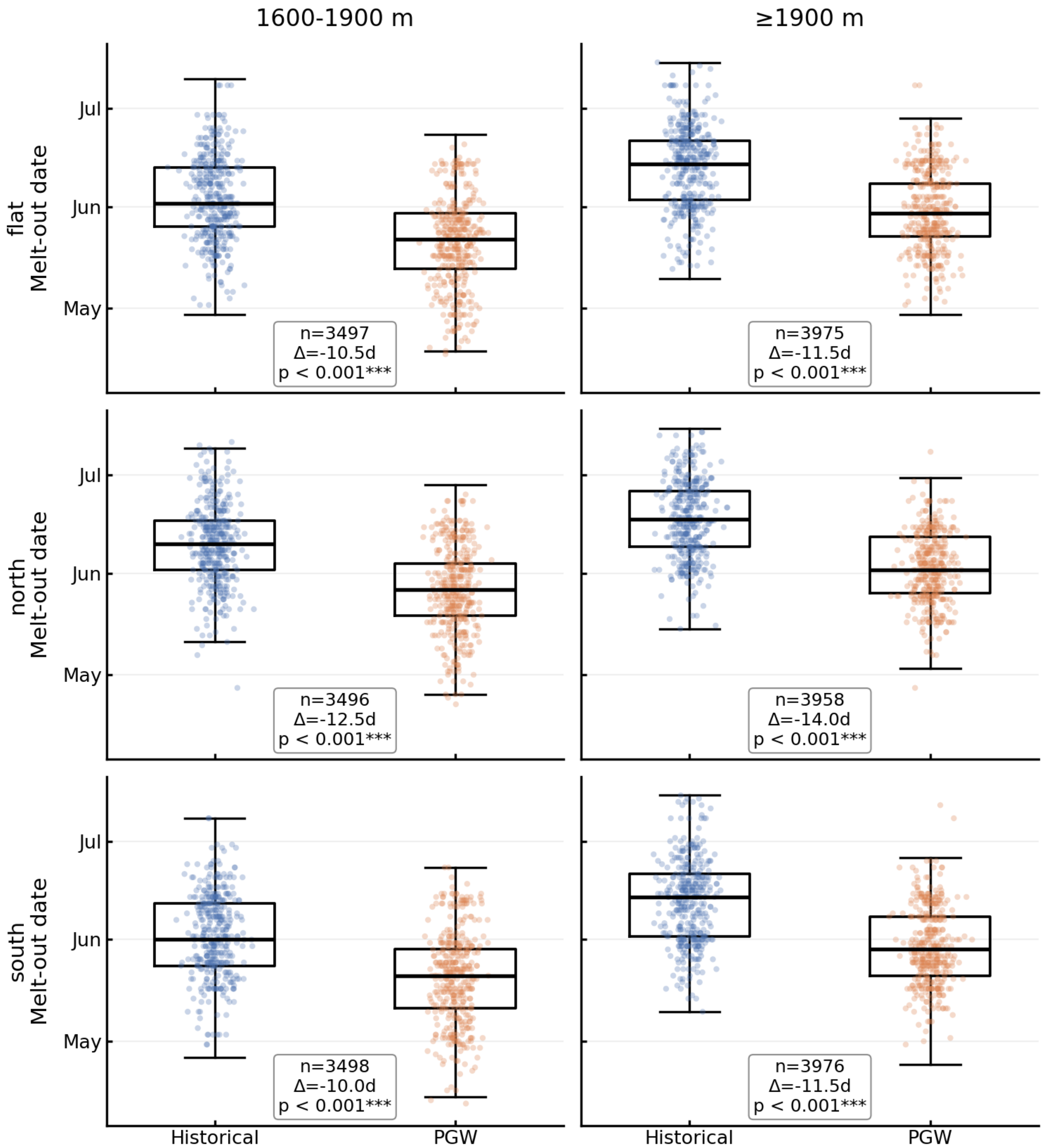

Figure 3: Melt-out date (month of year) under the historical and PGW simulations, for three terrain aspects (flat, north-facing, south-facing; rows) and two elevation bands (1,600–1,900 m, ≥1,900 m; columns), pooled across all 44 matched seasons. Boxes show the median and interquartile range with a jittered strip of individual grid-cell/season values (blue: historical; orange: PGW). Inset statistics report the pooled sample size (n), the median PGW−historical shift (Δ, days), and the p-value from a one-sample Wilcoxon signed-rank test on each grid cell's own across-season median shift. Melt-out advances significantly under PGW in all six panels ($\Delta = -10.0$ to -14.0 days; $p < 0.001$), with the largest advances at the upper elevation band on north-facing slopes.

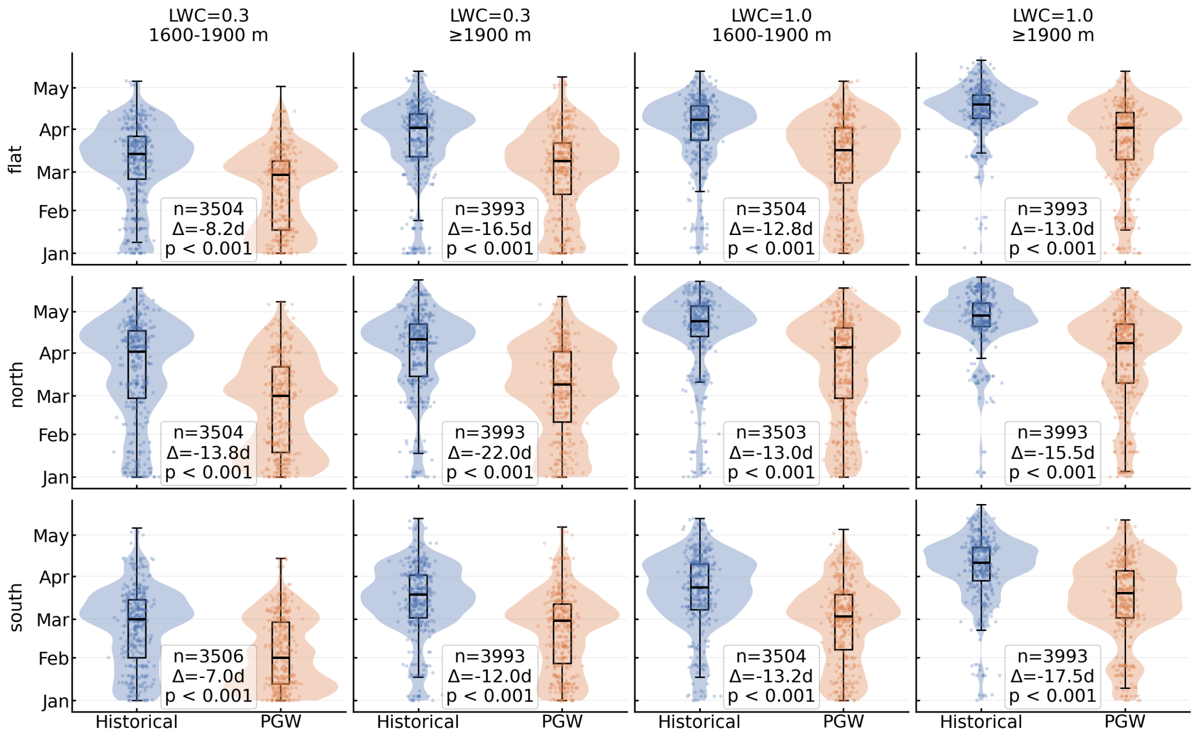

Figure 4: LWC_{index} threshold-crossing date (month of year) under historical and PGW simulations, for three terrain aspects (flat, north-facing, south-facing; rows) and the combination of two LWC_{index} thresholds (0.3, 1.0) and two elevation bands (1,600–1,900 m, $\geq$1,900 m; columns). Violins show the full distribution with an overlaid boxplot and a jittered strip of individual grid-cell/season values pooled across all 44 matched seasons (blue: historical; orange: PGW). Inset statistics report the pooled sample size (n), median PGW$-$historical shift (Δ, days), and p-value from a one-sample Wilcoxon signed-rank test on each grid cell's own across-season median shift. All twelve panels show a significant advance under PGW ($p < 0.001$), largest for the LWC$= 0.3$ threshold on north-facing terrain at the upper elevation band ($\Delta = -22.0$ days).

and LWC infiltration, which in turn governs wet snow avalanche release. Our results are limited to one study site, Glacier National Park, Montana, so we do not yet know whether this pattern holds in other snow climates in the western United States. Future research could investigate wet snow conducive conditions across continental and maritime snow climates in the western United States.

5. CONCLUSION

The results demonstrate a significant PGW-driven shift for all simulated variables – HS_{max}, melt-out day and LWC_{index} – for both elevation bands and all tested aspects. This implies that perturbed temperatures and precipitation reduce snow depth and move the onset of melt-out and wet snow avalanche conditions earlier in the year toward the mid-century. The detected shift is largest on north-facing slopes. For practitioners, this means our winters may become shorter, and wet snow conditions will likely occur earlier in the season (up to 22 days earlier in high elevations on north facing slopes). These results can support and inform operations that historically had closed prior to the onset of wet snow avalanche problems.

This study represents one small step toward closing the aspect-dependency knowledge gap and identifying the effect of climate change on wet snow avalanche cycles. Our conclusions should be interpreted conservatively given the model uncertainties, as well as the limitation of PGW methods in holding large-scale circulation patterns fixed while perturbing the thermodynamic profile alone.

DISCLAIMER

Any use of trade, firm, or product names is for descriptive purposes only and does not imply endorsement by the U.S. Government.

ACKNOWLEDGEMENTS

The authors thank Florence Miller for supporting us with snow height data from Flattop Mountain SNOTEL. Further, we thank Ron Simenhois, Florian Herla, Simon Horton, Michi Binder and Michael Reisecker for advancing post-processing for the SNOWPACK outputs and their knowledge exchange. We are grateful to Marianne Cowherd and Will McDermott for reviewing this manuscript. This work was supported by the U.S. Geological Survey North Central Climate Adaptation Science Center and the Ecosystems Land Change Science Program. This research employed a variety of AI tools: generative AI for manuscript editing, and AI-assisted coding for data processing. All AI-generated outputs, including text, code, and analytical results, were reviewed, validated, and, where necessary, modified by the authors to ensure scientific rigor, integrity, accuracy, and compliance with USGS standards.

REFERENCES

Adachi, S. A., Nishizawa, S., Yoshida, R., Yamaura, T., Ando, K., Yashiro, H., Kajikawa, Y., and Tomita, H. (2017). Contributions of changes in climatology and perturbation and the resulting nonlinearity to regional climate change. In: Nature Communications 8, p. 2224. https://doi.org/10.1038/s41467-017-02360-z.

Bartelt, P. and Lehning, M. (2002). A physical SNOWPACK model for the Swiss avalanche warning: Part I: numerical model. In: Cold Regions Science and Technology 35.3, pp. 123–145.

Brogli, R., Heim, C., Mensch, J., Sørland, S. L., and Schär, C. (2023). The pseudo-global-warming (PGW) approach: methodology, software package PGW4ERA5 v1.1, validation, and sensitivity analyses. In: Geoscientific Model Development 16.3, pp. 907–926. https://doi.org/10.5194/gmd-16-907-2023.

Buisan, S. T., Lopez-Moreno, J. I., Saz, M. A., and Kochendorfer, J. (2016). Impact of weather type variability on winter precipitation, temperature and annual snowpack in the Spanish Pyrenees. In: Climate Research 69, pp. 79–92.

Castebrunet, H., Eckert, N., Giraud, G., Durand, Y., and Morin, S. (Sept. 15, 2014). Projected changes of snow conditions and avalanche activity in a warming climate: the French Alps over the 2020–2050 and 2070–2100 periods. In: The Cryosphere 8.5, pp. 1673–1697. ISSN: 1994-0416. https://doi.org/10.5194/tc-8-1673-2014.

Eckert, N., Corona, C., Giacona, F., Gaume, J., Mayer, S., Herwijnen, A. van, Hagenmuller, P., and Stoffel, M. (May 2024). Climate change impacts on snow avalanche activity and related risks. In: Nature Reviews Earth & Environment 5.5, pp. 369–389. ISSN: 2662-138X. https://doi.org/10.1038/s43017-024-00540-2.

Evan, A. and Eisenman, I. (2021). A mechanism for regional variations in snowpack melt under rising temperature. In: Nature Climate Change 11.4, pp. 326–330.

Hägeli, P. and McClung, D. M. (2003). Avalanche characteristics of a transitional snow climate—Columbia Mountains, British Columbia, Canada. In: Cold Regions Science and Technology 37.3, pp. 255–276.

Hale, K. E., Jennings, K. S., Musselman, K. N., Livneh, B., and Molotch, N. P. (May 22, 2023). Recent decreases in snow water storage in western North America. In: Communications Earth & Environment 4.1. ISSN: 2662-4435. https://doi.org/10.1038/s43247-023-00751-3.

Hao, J., Zhang, X., Cui, P., Li, L., Wang, Y., Zhang, G., and Li, C. (Aug. 1, 2023). Impacts of Climate Change on Snow Avalanche Activity Along a Transportation Corridor in the Tianshan Mountains. In: International Journal of Disaster Risk Science 14.4, pp. 510–522. ISSN: 2192-6395. https://doi.org/10.1007/s13753-023-00475-0.

He, C., Valayamkunnath, P., Barlage, M., Chen, F., Gochis, D., Cabell, R., Schneider, T., Rasmussen, R., Niu, G.-Y., Yang, Z.-L., et al. (2023). Modernizing the open-source community Noah with multi-parameterization options (Noah-MP) land surface model (version 5.0) with enhanced modularity, interoperability, and applicability. In: Geoscientific Model Development 16.17, pp. 5131–5151.

Hersbach, H., Bell, B., Berrisford, P., Hirahara, S., Horányi, A., Muñoz-Sabater, J., Nicolas, J., Peubey, C., Radu, R., Schepers, D., et al. (2020). The ERA5 global reanalysis. In: Quarterly journal of the royal meteorological society 146.730, pp. 1999–2049.

Kruyt, B., Wever, N., Mayer, S., and Vergara, J. T. (2023). Avalanche activity in a changing climate: Changes in wet and dry slab avalanches based on climate simulations over Switzerland. In: Proceedings International Snow Science Workshop.

Lazar, B. and Williams, M. (Feb. 2008). Climate change in western ski areas: Potential changes in the timing of wet avalanches and snow quality for the Aspen ski area in the years 2030 and 2100. In: Cold Regions Science and Technology 51.2, pp. 219–228. ISSN: 0165232X. https://doi.org/10.1016/j.coldregions.2007.03.015.

Lehning, M., Bartelt, P., Brown, B., Fierz, C., and Satyawali, P. (2002). A physical SNOWPACK model for the Swiss avalanche warning: Part II. Snow microstructure. In: Cold regions science and technology 35.3, pp. 147–167.

López-Moreno, J. I., Revuelto, J., Gilaberte, M., Morán-Tejeda, E., Pons, M., Jover, E., Esteban, P., García, C., and Pomeroy, J. (2014). The effect of slope aspect on the response of snowpack to climate warming in the Pyrenees: JI López-Moreno et al. In: Theoretical and Applied Climatology 117.1, pp. 207–219.

Mayer, S., Hendrick, M., Michel, A., Richter, B., Schweizer, J., Wernli, H., and Van Herwijnen, A. (May 7, 2024). Changes in snow avalanche activity in response to climate warming in the Swiss Alps. https://doi.org/10.5194/egusphere-2024-1026.

Mitterer, C., Heilig, A., Schmid, L., Herwijnen, A. van, Eisen, O., and Schweizer, J. (2016). “Comparison of measured and modelled snow cover liquid water content to improve local wet-snow avalanche prediction”. In: International Snow Science Workshop Proceedings. Vol. 5.

Mitterer, C., Techel, F., Fierz, C., and Schweizer, J. (2013). “An operational supporting tool for assessing wet-snow avalanche danger”. In: Proceedings ISSW. Vol. 33, pp. 334–338.

Mock, C. J. and Birkeland, K. W. (2000). Snow avalanche climatology of the western United States mountain ranges. In: Bulletin of the American Meteorological Society 81.10, pp. 2367–2392.

National Park Service (2026). Weather - Glacier National Park. `https://www.nps.gov/glac/learn/nature/weather.htm`. Accessed: July 9, 2026.

Newton, B. W., Farjad, B., and Orwin, J. F. (Jan. 2021). Spatial and Temporal Shifts in Historic and Future Temperature and Precipitation Patterns Related to Snow Accumulation and Melt Regimes in Alberta, Canada. In: Water 13.8, p. 1013. ISSN: 2073-4441.

O'Neill, B. C., Tebaldi, C., Van Vuuren, D. P., Eyring, V., Friedlingstein, P., Hurtt, G., Knutti, R., Kriegler, E., Lamarque, J.-F., Lowe, J., et al. (2016). The scenario model intercomparison project (ScenarioMIP) for CMIP6. In: Geoscientific Model Development 9.9, pp. 3461–3482.

Peitzsch, E. H., Martin, J., Greene, E., Eckert, N., Favillier, A., Konigsberg, J., Kichas, N., Stahle, D., Birkeland, K., Elder, K., and Pederson, G. (June 24, 2025). Changing drivers of regional large magnitude avalanche frequency throughout Colorado, USA. https://doi.org/10.5194/egusphere-2025-2217.

Peitzsch, E. H., Pederson, G. T., Birkeland, K. W., Hendrikx, J., and Fagre, D. B. (May 11, 2021). Climate drivers of large magnitude snow avalanche years in the U.S. northern Rocky Mountains. In: Scientific Reports 11.1, p. 10032. ISSN: 2045-2322. https://doi.org/10.1038/s41598-021-89547-z.

Pielmeier, C., Techel, F., Marty, C., and Stucki, T. (2013). "Wet snow avalanche activity in the Swiss Alps–trend analysis for mid-winter season". In: Proceedings of the international snow science workshop, grenoble and chamonix, pp. 1240–1246.

Rasmussen, R. M., Chen, F., Liu, C., Ikeda, K., Prein, A. F., Kim, J.-H., Schneider, T. L., Dai, A., Gochis, D. J., Dugger, A. L., et al. (2023). CONUS404: Four-kilometer long-term regional hydroclimate reanalysis over the conterminous United States (ver. 2.0, December 2023). In: US Geological Survey (USGS) Data Release, p. 207.

Reuter, B., Hagenmuller, P., and Eckert, N. (2025). Trends in avalanche problems in the French Alps between 1958 and 2020. In: Cold Regions Science and Technology 238, p. 104555.

Riahi, K., Van Vuuren, D. P., Kriegler, E., Edmonds, J., O'neill, B. C., Fujimori, S., Bauer, N., Calvin, K., Dellink, R., Fricko, O., et al. (2017). The Shared Socioeconomic Pathways and their energy, land use, and greenhouse gas emissions implications: An overview. In: Global environmental change 42, pp. 153–168.

Rodgers, K. B., Lee, S.-S., Rosenbloom, N., Timmermann, A., Danabasoglu, G., Deser, C., Edwards, J., Kim, J.-E., Simpson, I., Stein, K., et al. (2021). Ubiquity of human-induced changes in climate variability. In: Earth System Dynamics Discussions 2021, pp. 1–22.

Synoptic Data PBC (2026). Station LGPVC: Basic Weather Observations. https://viewer.synopticdata.com/metadata/LGPVC/basic-weather/now. Accessed: 2026-08-11. Synoptic Data PBC.

USDA Natural Resources Conservation Service (2026). Flattop Mtn. (482) - Site Information and Reports. National Water and Climate Center (NWCC) SNOTEL Site, Montana. Accessed 2026-07-10.

Wever, N., Fierz, C., Mitterer, C., Hirashima, H., and Lehning, M. (2014). Solving Richards Equation for snow improves snowpack meltwater runoff estimations in detailed multilayer snowpack model. In: The Cryosphere 8.1, pp. 257–274.

Wever, N., Schmid, L., Heilig, A., Eisen, O., Fierz, C., and Lehning, M. (2015). Verification of the multi-layer SNOWPACK model with different water transport schemes. In: The Cryosphere 9.6, pp. 2271–2293.

Wilcoxon, F. (1945). Individual comparisons by ranking methods. In: Biometrics bulletin 1.6, pp. 80–83.

WSL Institute for Snow and Avalanche Research SLF (2026). SNOWPACK (Version commit 77c94a0e). https://gitlabext.wsl.ch/snow-models/snowpack/-/commit/77c94a0ead2fb93e5d4b0d06dfe563f085bcc3bf. Accessed 25 June 2026; commit authored by Nander Wever.

Xue, L., Rasmussen, R. M., Chen, F., Liu, C., Ikeda, K., Prein, A., Kim, J.-H., Schneider, T. L., Dai, A., Gochis, D., et al. (2024). Four-kilometer long-term regional hydroclimate forecast over the conterminous United States (CONUS). In: US Geological Survey (USGS) Data Release, p. 1267.

Xue, Z., Ullrich, P., and Leung, L.-Y. R. (2023). Sensitivity of the pseudo-global warming method under flood conditions: a case study from the northeastern US. In: Hydrology and Earth System Sciences 27.9, pp. 1909–1927.